2016-01-2160
Published 10/17/2016

doi:10.4271/2016-01-2160
saeeng.saejournals.org

The Effects of Cylinder Deactivation on the Thermal Behaviour and Performance of a Three Cylinder Spark Ignition Engine

Alexander Bech, Paul J. Shayler, and Michael McGhee
University of Nottingham

ABSTRACT

A physics based, lumped thermal capacity model of a 1litre, 3 cylinder, turbocharged, directly injected spark ignition engine has been developed to investigate the effects of cylinder deactivation on the thermal behaviour and fuel economy of small capacity, 3 cylinder engines. When one is deactivated, the output of the two firing cylinders is increased by 50%. The largest temperature differences resulting from this are between exhaust ports and between the upper parts of liners of the deactivated cylinder and the adjacent firing cylinder. These differences increase with load. The deactivated cylinder liner cools to near-coolant temperature. Temperatures in the lower engine structure show little response to deactivation. Temperature response times following deactivation or reactivation events are similar. Motoring work for the deactivated cylinder is a minor loss; the net benefit of deactivation diminishes with increasing load. For the NEDC and FTP-75 cycle, the predicted fuel savings are ~3½ %; the benefit is lower for more transient or highly loaded cycles.

CITATION: Bech, A., Shayler, P., and McGhee, M., "The Effects of Cylinder Deactivation on the Thermal Behaviour and Performance of a Three Cylinder Spark Ignition Engine," *SAE Int. J. Engines* 9(4):2016, doi:10.4271/2016-01-2160.

INTRODUCTION

In recent years, the downsizing of direct injection spark ignition engines for light duty automotive applications has made a major contribution to improving the fuel economy of private passenger vehicles. Turbocharging and direct injection fuelling have been key technologies which allow smaller capacity engines to be used to meet required power and torque output requirements. These smaller engines operate at higher cylinder mean effective pressures across the load range than the engines they supersede. At part-load, throttling losses are reduced, gross indicated thermal efficiency is improved and reductions in engine capacity reduce friction power losses. The improvements under part-load conditions make a strong contribution to improving vehicle fuel consumption over drive cycles such as the New European Drive Cycle (NEDC).

Downsized engines with a swept capacity of around 1.0litre are most commonly three-cylinder designs. Further downsizing by reducing cylinder capacity or the number of cylinders is possible, but other directions of technical innovation may be preferred for the next generation of small engines. One area of technology receiving attention is cylinder deactivation as a means of reducing the effective cylinder displacement for light load operation. Past applications in the automotive area have commonly been to relatively large displacement engines with six or more cylinders [1, 2, 3, 4, 5, 6, 7, 8]. Since 2012, however, VW have produced a 1.4l, 4 cylinder TSI engine with Active Cylinder Technology [2]. This enables the deactivation of two of the four cylinders within an envelope of light load operating conditions. Ford have also reported exploring the application of cylinder deactivation to the three cylinder 1.0l Ford EcoBoost engine [3],[9].

Various systems for deactivating cylinders have been described in the literature, including systems which eliminate piston reciprocation to reduce friction [10] or deactivate all cylinders in turn in a pattern which minimises temperature changes [2]. Most commonly however, cylinder deactivation is applied to particular cylinders and achieved by cutting fuel supply and disabling intake and exhaust valve actuation, leaving the valves closed. Depending on the timing of the disablement, the trapped cylinder gas can be predominantly air or products of combustion [1]. The various means of achieving disablement include the use of switchable roller tappets, switchable rocker arms, and camshaft shifting systems [1]. Fuel economy improvements are attributed to reductions in pumping work and an increase in gross indicated thermal efficiency [11]. Reported improvements in fuel economy are significant, ranging from a maximum of 30-40% for a 2.0l V6 carburetted petrol engine [12] when deactivating a bank of cylinders at low loads, to 25% for the 1.4l TSI [2] at low loads, and 6-10% for a 1.4l four-cylinder turbocharged engine with one or two cylinders deactivated [13].

The application of cylinder deactivation to three cylinder, 1 litre engines is a departure from the norm and present challenges which include the uncertain effects on thermal behaviour of deactivating one of three cylinders. An investigation of these effects through computational modelling and experimental studies is reported in the paper. The model is a variant of the PROMETS [14] code describing thermal behaviour in the engine structure using a lumped thermal capacity approach with sub-models representing friction, interactions with coolant and oil, and gas exchange processes. These and the

representation of losses associated with a motored deactivated cylinder are outlined, and the fuel economy benefits of deactivation investigated.

MODEL FEATURES

The computational model used in the work is a variant of PROMETS [14], in which the engine structure is modelled using 41 lumped thermal capacity elements per cylinder. This is combined with models of internal and external coolant loops, as shown in Figure 1, and the oil circuit. The model has a set of physics based sub models carried over with some revisions from previous applications. These describe friction characteristics [15], local heat transfer conditions for heat exchange between the engine structure [16], coolant [17] and oil, gas-side heat transfer to the combustion system walls and heat exchange in the intake and exhaust ports [18] [19] .

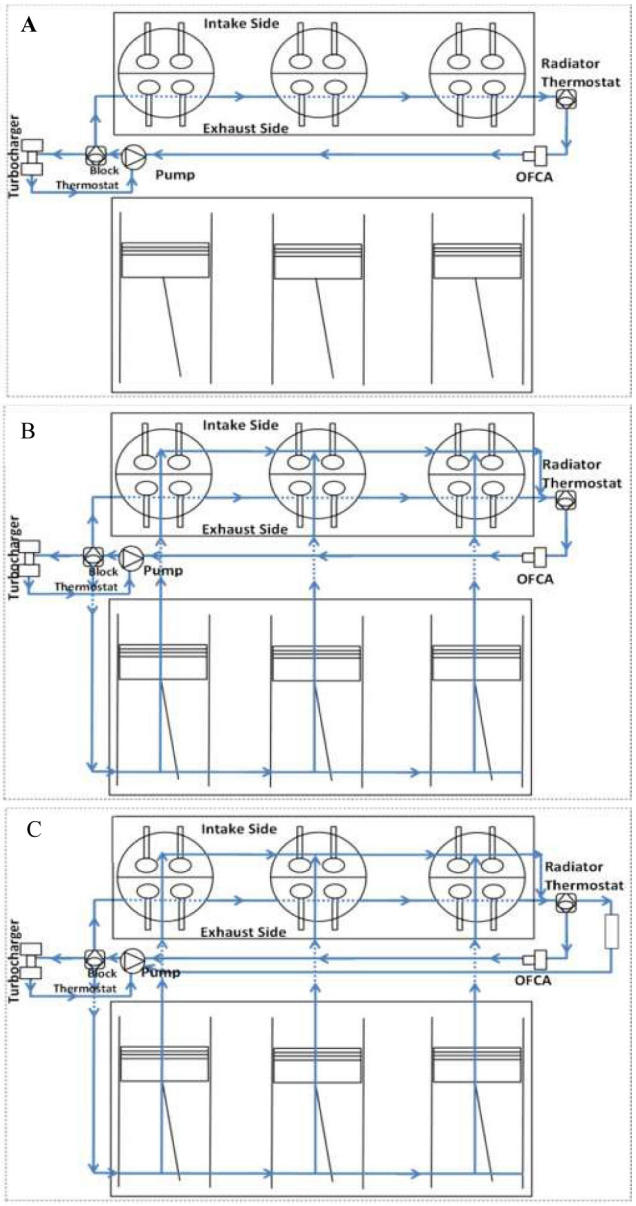

Figure 1. Coolant schematic for the modelled three cylinder engine [A] prior to the block thermostat opening, [B] after the block thermostat opens and [C] when the radiator thermostat opens.

A version of the 3 cylinder engine with the same displacement but without cylinder deactivation technology provided information on component masses which were compared to values predicted by a pre-processor for PROMETS. After minor adjustments, agreement between the predicted masses of modelled engine components and measured values was good, as shown in Figure 2. The piston stroke is 82mm and the cylinder coolant jacket extends to 65mm from the top of the block. The engine has an integrated exhaust manifold which was represented in simplified form which reproduced the surface area and internal volume and length of the manifold tracts by reference to CAD drawings.

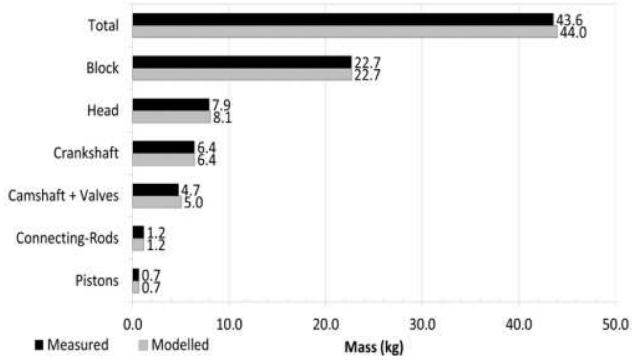

Figure 2. Comparison of measured and modelled masses for core elements representing the modelled engine build.

The cooling system of the engine passes through three modes of operation controlled by two thermostats as it warms up. These are illustrated in Figure 1. In the early stages of warm-up, coolant in the block is in a quiescent condition and coolant is circulated through the exhaust side of the head, as in (A), and returned to pump inlet through an external bypass. In the second mode (B), the first, head thermostat opens and there is forced circulation of coolant through both the head and the block. Finally, when the coolant reaches its fully warm temperature, the second thermostat opens and the system operates as shown in (C), allowing coolant circulation through the radiator.

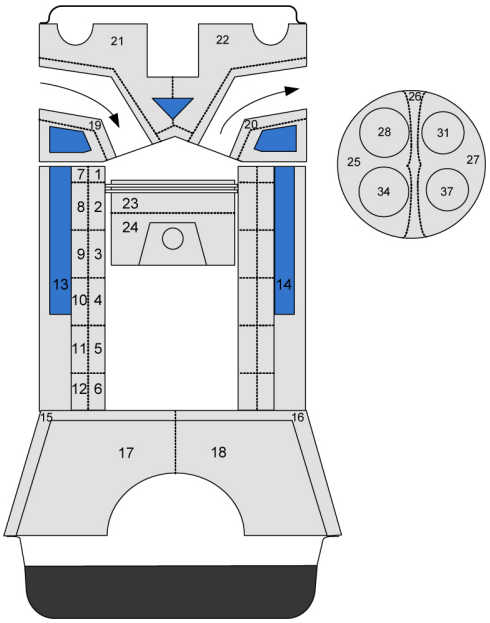

Figure 3. Side-view (left) representation of the block, head and piston components in the thermal model. (Right) Bottom-view representation of the cylinder head and intake and exhaust valve head element numbers.

An example of the modelled representation for one of the three cylinders is shown in Figure 3.

Friction and Ancillaries

The total combined rubbing friction and ancillary loads of the engine without cylinder deactivation were determined experimentally from the difference between net IMEP and BMEP over a range of engine operating conditions. The engine was run with an oil fill which meets the SAE 5W-20 specification. The corresponding friction prediction was increased by 10% to match the experimentally measured value, with each component contribution scaled by the same factor. The friction model is described in [15]. The agreement between measured and adjusted prediction of the total and the distribution between contributing sources are shown in Figure 4 as a variation with engine speed.

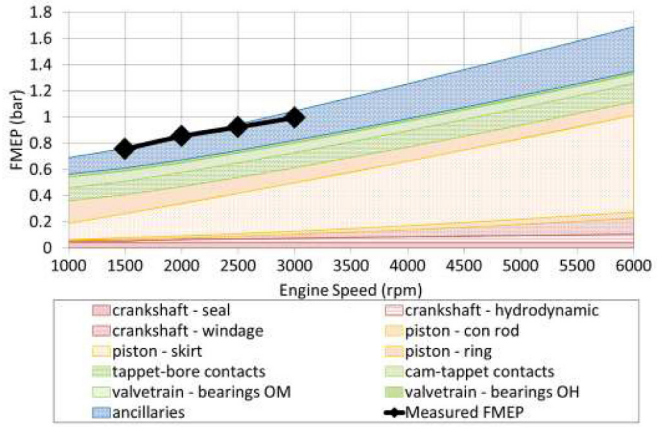

Figure 4. Modelled and measured FMEP values for fully warm conditions, i.e. i.e. T_{oil} = 90°C for a flat-follower configuration.

Losses Associated with Motoring a Deactivated Cylinder

The form of cylinder deactivation considered here shuts off gas exchange by leaving intake and exhaust valves closed [21] [22], effectively sealing the cylinder, and disables fuel injection electronically. The trapped gas in the cylinder is compressed and expanded every engine revolution. The compression and expansion processes adjust within a small number of cycles to establish repeating closed pressure-volume figures. The cylinders are not perfectly sealed due to piston blow-by and leakage passed valves. Gas transfer occurs out of the cylinder when cylinder pressure is high and into the cylinder when pressure is low. This gas exchange represents a small fraction of the cylinder mass and does not noticeably distort the compression and expansion processes which can be treated as polytropic processes with different values of the polytropic index. The work required to motor the deactivated cylinder represents a performance penalty which should be accounted for in weighing the benefits and disadvantages of deactivation, although Leone et al [4] reported the work penalty is small, representing a penalty of around 0.02 bar IMEP.

In the current work, experimental measurements of the pressure variation in a deactivated cylinder show that it takes typically 30 \ engine revolutions to adjust to a repeating pattern. The mass trapped on the first deactivated cycle depends on the timing of valve closure in the cycle. Dependent on this, there is a reduction in trapped mass of up to 70% due to blowby during the settling period. An example of the stabilised pressure variation is given in Figure 5. The compression and expansion lines almost overlay, indicating almost all the work done during compression is recovered during the expansion stroke, and the linearity of the.process lines indicate these are polytropic with a similar polytropic index value. The penalty due to pumping air requires 2-3 Joules per revolution, which is equivalent to 0.02-0.03 bar IMEP, and similar to the losses reported in [4]. This is a minor loss but note however, that the deactivated cylinder continues to reciprocate and makes a larger contribution to the engine rubbing friction.

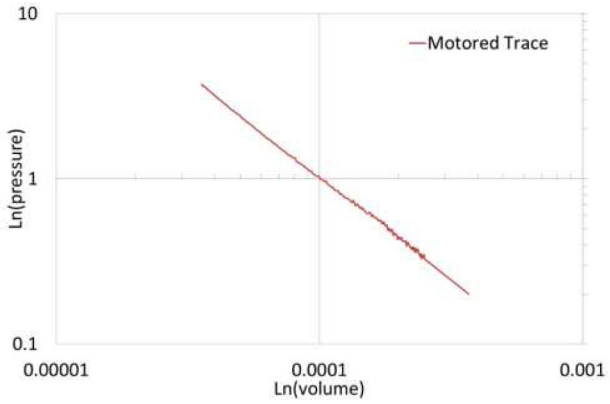

Figure 5. Measured stabilised pressure trace for a motored cylinder (1500rpm, 20Nm).

Neglecting the losses associated with mass transfer into and out of the cylinder after the early transient conditions have settled, the dissipated work per revolution is the difference between work done on the trapped gas during the compression and expansion strokes. Because this difference is small, a direct calculation is badly conditioned to small errors in the values of the polytropic indices. More robustly, the total work dissipated can be equated to the heat transferred from the gas. The direction and magnitude of heat transfer are the same for both the compression and expansion strokes, and over the two strokes is approximately twice the heat transfer during the compression stroke. As shown in Appendix 1, treating the trapped charge as a perfect gas and the cylinder as a closed system, the dissipated work over the two strokes

$$\oint W = -\oint Q_{rev,n} = -2mR\Delta T\left(\frac{\gamma - n}{(\gamma - 1)(n - 1)}\right)$$

To evaluate this, an estimate of the trapped mass, m, and gas temperature change ΔT over the stroke, and the polytropic index n are required. Values of n determined from pressure -volume diagrams were in the range 1.34-1.36. The trapped mass was estimated using the perfect gas equation and air properties. The biggest uncertainty is

in the value of cylinder gas temperature, as this is not measured at any point in the cycle. Here it is assumed that at BDC piston position, the gas temperature is close to wall temperature and the surrounding coolant temperature, and taken to be 400K. With this assumption and using the average index value, 1.35, the work dissipation was calculated to be 2.2-3.2 J/rev, which is consistent with the values given in [4] and small enough to be considered a minor loss.

Gas Exchange Processes

Deactivating one cylinder requires an increase in work output of 50% from the other two to maintain the same engine brake output. If mixture AFR is stoichiometric, the air flow to each of the two firing cylinders also increases by close to 50%. (The increase is less than half if fuel economy has been improved by deactivating the third cylinder). The increase in airflow reflects any change in cylinder volumetric efficiency resulting from the change in operating point of the two firing cylinders, and a reduction in throttling loss which raises intake port pressure and reduces pumping work. The reduction reduces the net indicated work required for a given brake work output and accounts for most of any improvement in fuel economy at light load. The pumping work is proportional to the difference between intake port and exhaust port pressures. The exhaust port pressure depends upon the change in cylinder volumetric efficiency, turbocharger system design, control strategy and calibration details. In the current study, cylinder volumetric efficiency and exhaust pressure were defined empirically for the range of operating conditions covered by the NEDC and FTP-75 drive cycle by reference to data taken with the engine operating without cylinder deactivation. Cylinder volumetric efficiency was defined as a corrected ideal value dependent upon compression ratio, engine speed and intake and exhaust back pressure. A comparison of the experimental data for cylinder volumetric efficiency with the engine running on three cylinders and the simulated variation is given in Figure 6. The difference between the experimental and simulated results is generally less than 5%. Discrepancies were higher for idling (-8%) and, because the transient effects such as manifold filling were neglected, following rapid throttle opening or closing. The same function for cylinder volumetric efficiency was applied to the firing cylinders when running with the third cylinder deactivated. The exhaust back pressure was similarly defined by reference to the experimental data for three cylinder operation, as a function of engine total airflow and waste gate position. The small change in the total engine air flow consumption between two and three cylinder operation at the same brake output work and engine speed was neglected, and the turbocharger was assumed to be unaffected by the change in exhaust pulse frequency. Using the empirical functions to describe cylinder volumetric efficiency and exhaust back pressure, the cumulative pumping work over the NEDC was measured to be 0.243 kWh compared to the function value of 0.247kWh (1.6% difference). For the FTP-75 cycle the corresponding values were 0.381kWh and 0.339kWh respectively (-11.1% difference). A comparison of second- by- second variation in PMEP is given in Figure 7 A for the NEDC and Figure 6B for the FTP-75.

Instantaneous fuel consumption was determined from experimental values of gross indicated specific fuel consumption (per cylinder) and the sum of simulated pumping work, friction and ancillary work, the loss associated with motoring a deactivated cylinder, and the brake output work. The indicated load is weakly dependent on fuel consumption, so a simple iteration is required to solve for fuel consumption and indicated load values which are self- consistent. Comparisons of experimental and simulation results for instantaneous and cumulative fuel consumption are given in Figure 8. For these comparisons, the experimental variations of bulk coolant and bulk oil temperatures were used in the simulations to avoid possible confounding of the reasons for discrepancies; as illustrated, the agreement between measured and simulated cumulative fuel consumption is good for both drive cycles.

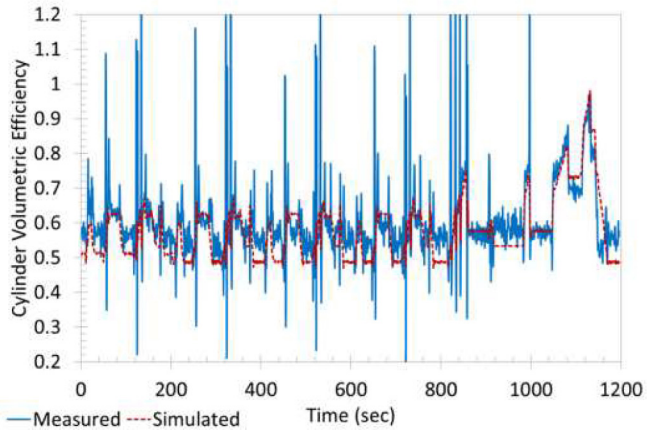

Figure 6. Comparison of modelled and experimental cylinder volumetric efficiency for the NEDC, for a cold start where $T_{coolant}$ = 20°C.

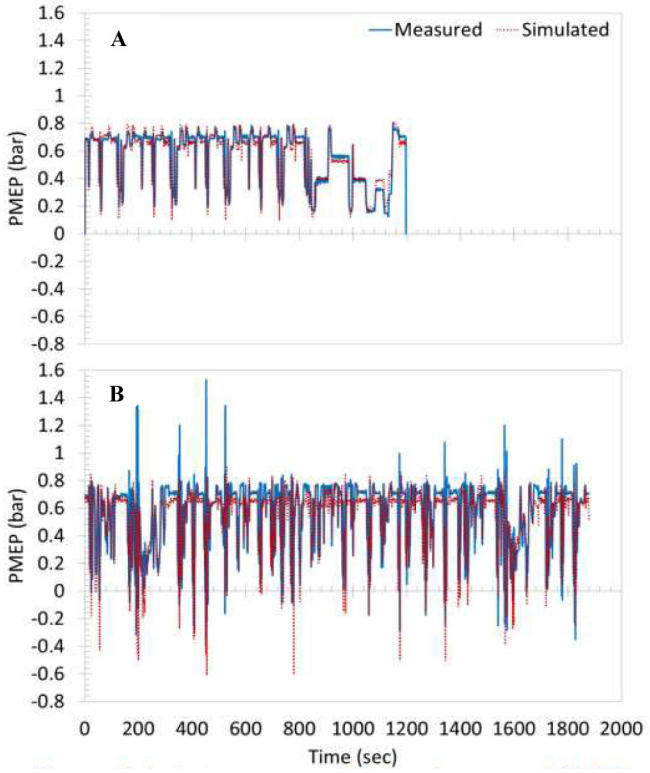

Figure 7. Instantaneous modelled and measured PMEP for (A) the NEDC and (B) FTP-75.

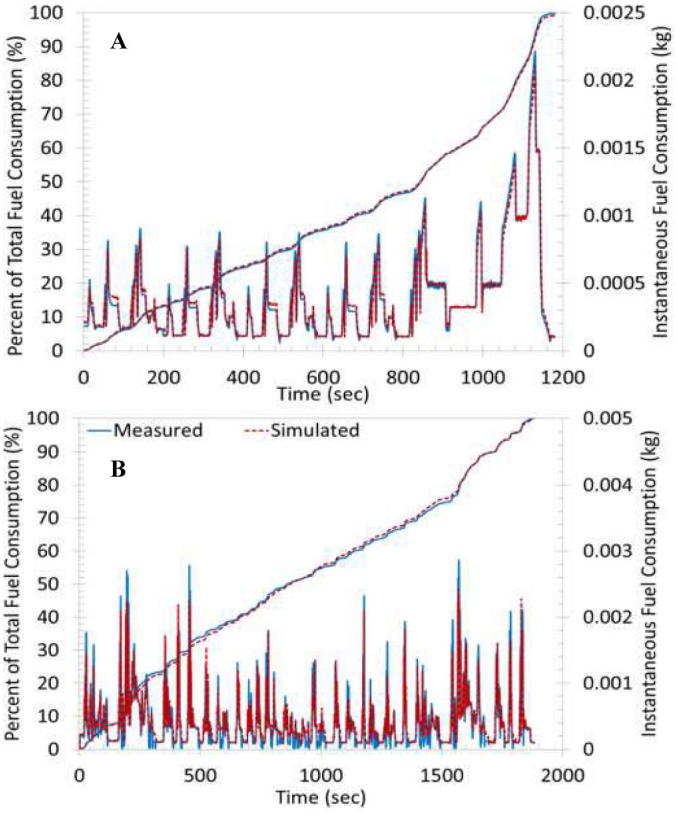

Figure 8. Simulated and experimental fuel consumption for the (A) NEDC and (B) FTP-75.

Thermocouple Locations in Test Engine

A variant of the engine without cylinder deactivation technology was used to validate model predictions of temperatures. 1.5mm K-Type thermocouples were used to measure intake and exhaust port metal temperatures, cylinder wall metal temperatures as well as coolant and oil temperatures. The overview of thermocouple locations in the head and block are shown in Figures 9 and 10 respectively.

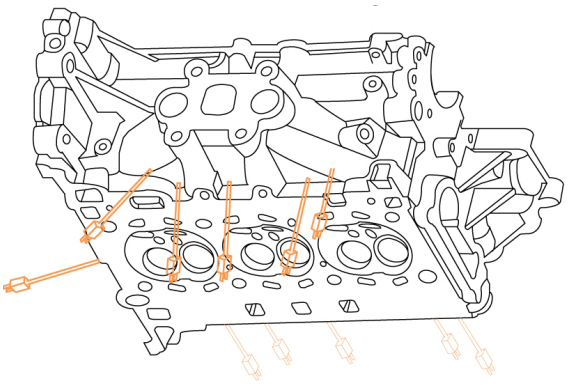

Figure 9. Line drawing of the cylinder head showing the locations of the thermocouples recording metal and coolant temperatures.

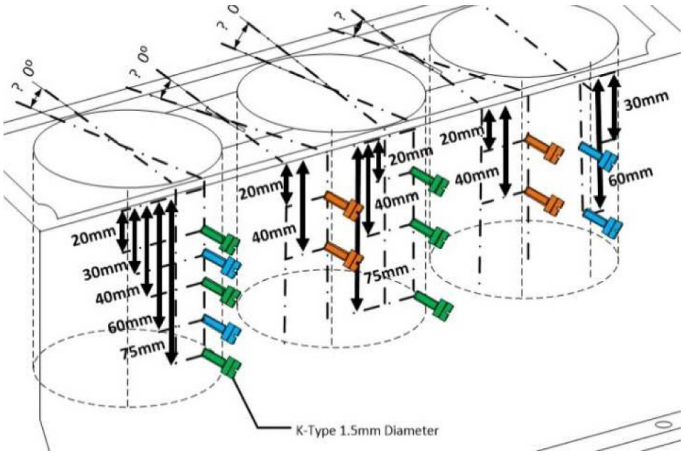

Figure 10. Thermocouple configurations for the block metal (green thermocouples), inter-bore (orange thermocouples) and coolant (blue thermocouples).

Thermal Behaviour

As warm-up progresses, the configuration of the engine coolant circuit is changed by the sequential opening of two thermostats as depicted in Figure 1. The rise of coolant temperature commonly leads the rise in oil temperature during warm-up. The warm-up variation in oil temperature is particularly important because it strongly influences engine friction and hence indicated load. Comparisons of predicted and experimental variations in oil and coolant temperatures over the NEDC are given in Figure 11. (A) shows the variation of oil temperature in the engine main oil gallery, (B) shows the coolant temperature in the block bypass to pump inlet and (C) the coolant temperature in the block. The agreement between predicted and experimental data is good, including the times at which the first and second thermostats open. The opening points at ~200s and ~900s respectively are marked by the changes in the rate of coolant temperature change which can be seen in (B) and (C).

Examples of measured and predicted cylinder wall temperatures under fully warm, steady operating conditions are given in Figure 12. These cover 1500rpm, 2000rpm and 3000rpm and brake loads from 20Nm to 80Nm. The right hand figures show results for the middle cylinder; agreement between predicted and measured temperatures is excellent. The left hand figures are for cylinder 1, which is correctly predicted to run slightly cooler. The agreement between predicted and measured temperatures is less good than for the middle cylinder,with predictions giving higher temperatures than measured values. However, the depth of the thermocouple tips in the cylinder walls is known only approximately, introducing some uncertainty, and over a wider range of operating conditions, the inter-cylinder temperature differences were predicted reasonably accurately as indicated in the comparison given in Table 1.

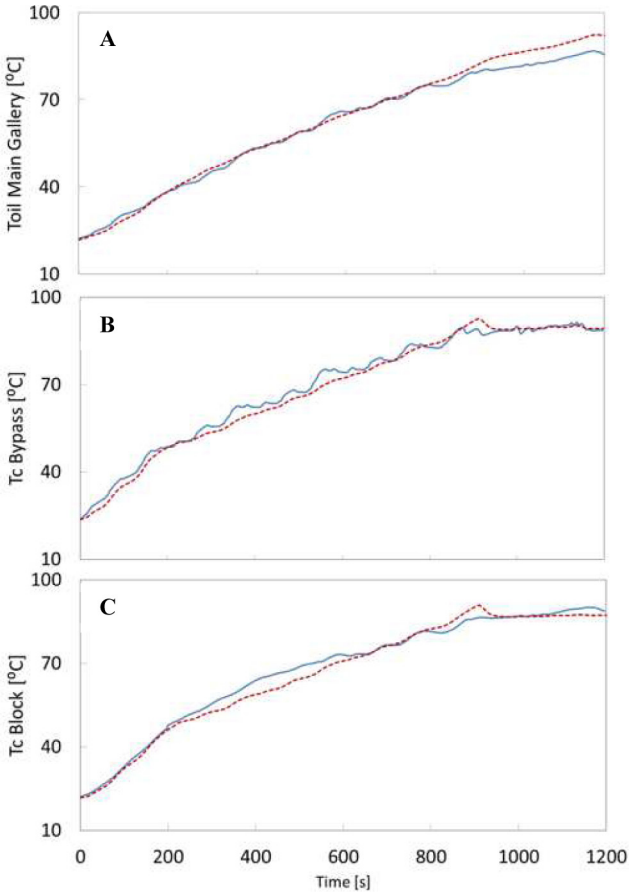

Figure 11. Modelled and experimental (A) oil main gallery, (B) bypass coolant and (C) block coolant passage warm-up rates for the NEDC (supplied by BP).

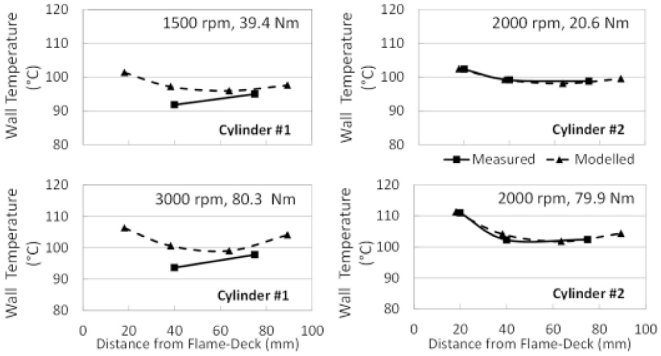

Figure 12. Measured and Modelled Cylinder Wall Metal Temperatures for Cylinder #1 and #2.

Table 1. Measured and Modelled Intake Port Metal Temperatures

Operating Condition		Measured/Predicted Temperatures			
		Cyl1	*Cyl2*	*Cyl3*	*Ave. diff.*
1500rpm	**20 Nm**	93.9/94.8	94.7/93.6	92.2/94.7	0.8
	60 Nm	96.7/100.6	97.3/99.5	93.5/97.2	3.3
3000rpm	**40 Nm**	95.8/101.6	96.4/100.7	93.9/96.8	4.3
	80 Nm	96.4/103.2	97.0/102.4	94.5/97.6	5.1

THERMAL RESPONSE TO CYLINDER DEACTIVATION

When operating with all three cylinders firing, temperature differences between the same locations on adjacent cylinders are generally contained to less than 3°C degrees at even half load as illustrated by the results given in Table 1. However, these differences increase substantially when one cylinder is deactivated and the work output from the other two is increased by 50% to maintain the same engine work output. The deactivated cylinder continues to reject heat generated by the motoring losses and rubbing friction at the piston-liner interface. However, the rate of heat rejection is relatively low and does not maintain the wall, piston or valve temperatures and after a period of adjustment these are lower. On the other hand, the firing cylinders reject more heat to the combustion system surfaces and piston, walls and valve temperatures increase. There is little information in the public domain to indicate the strength of these changes in thermal state, which have the potential to influence many aspects of engine performance.

The largest temperature differences occur between the deactivated cylinder and the adjacent firing cylinder. Predicted differences between a deactivated front cylinder (farthest from the flywheel, cylinder 1) and the centre, firing cylinder (cylinder 2) are shown in Figure 13 for three engine speeds and a load range up to a full load torque 170Nm; this range shows the trends clearly although in practice, the higher loads would not be accessible with a deactivated cylinder and fuel economy benefits are significant only at the lower end of the load range. The largest temperature differences are between the exhaust ports and between the top sections of the cylinder liners of the deactivated and firing cylinders. These are the areas where heat fluxes from the firing cylinder are highest. Differences are lower further down the liner, and in the near-valve area of the intake ports, which are preferentially warmed by the firing cylinder. Temperature differences in the cylinder head between the deactivated and firing cylinders are smaller than in the cylinder block. This is due to the greater moderating effect of the head coolant flow. The effect of deactivation on the lower parts of the engine is relatively weak.

Temperature distributions for all three cylinder liners are shown in Figure 14 for an operating condition of 2000rpm and 60Nm. This illustrates how the deactivated cylinder cools to the more uniform temperature, which is close to coolant temperature. Cylinder 1, the deactivated cylinder, cools to a near-uniform temperature. The variation in temperature differences between Cylinder 1 and Cylinder 2 largely follow from the temperature variation down the liner of Cylinder 2. Cylinder 3 operates at the highest temperatures, in part due to the direction of coolant circulation but primarily because Cylinder 2 is cooled by heat flow towards the deactivated cylinder. Regardless of load, the temperature of Cylinder 1 falls to near coolant temperature when deactivated. The corresponding rise in liner temperature of Cylinder 2 increases with engine load and are greatest near the top of the liner.

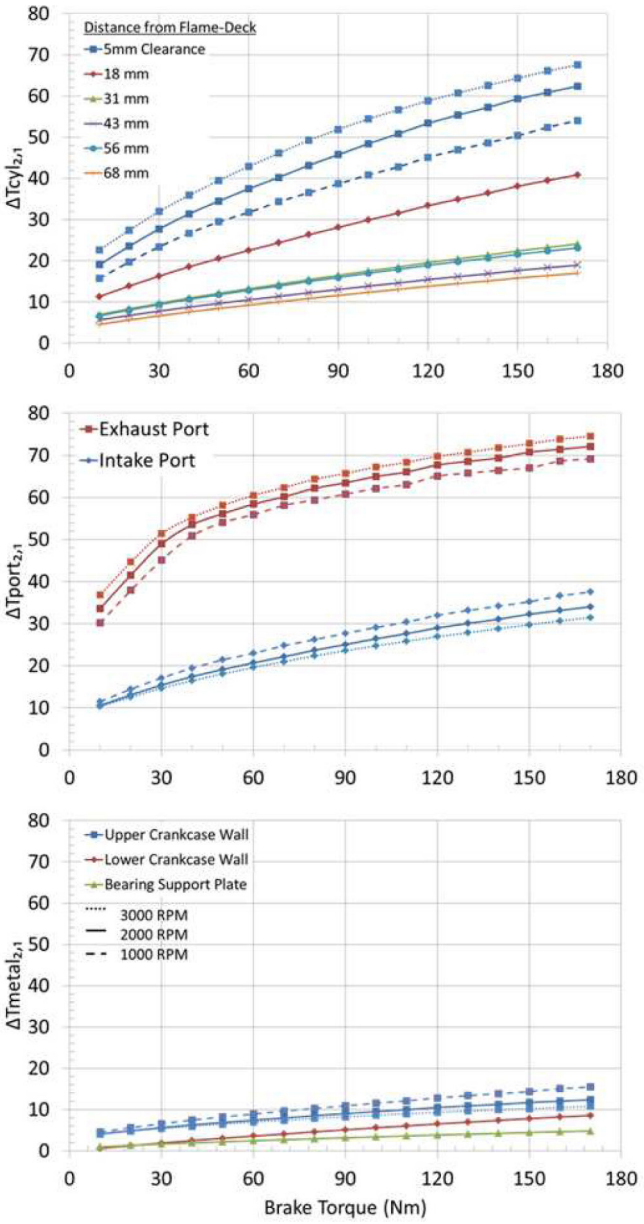

Figure 13. Modelled temperature difference between adjacent metal components between the deactivated and firing cylinder as a function of brake torque.

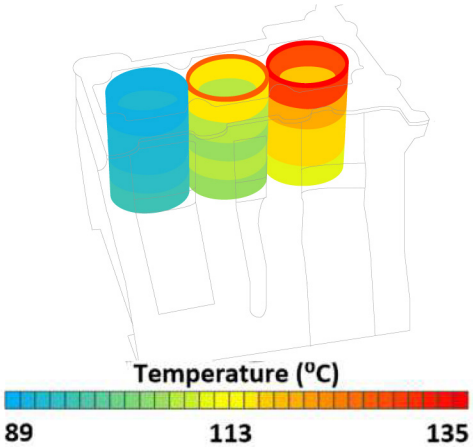

Figure 14. Modelled stabilised cylinder wall temperatures after deactivation; N=2000rpm and Tb= 60Nm.

Temperature Response Times

Following cylinder deactivation or reactivation events, the largest temperature changes occur in the upper section of the cylinder liner and the exhaust valve heads and lower stems. The times for temperatures to adjust to new steady values depend on the size of the temperature adjustment and local heat flows. The deactivated or reactivated cylinder undergoes the largest temperature changes, and the times required for temperatures to adjust are longest although the time constants are similar. An example of the upper liner temperature changes following deactivation and reactivation is given in Figure 15, and an illustration of the time dependent response is shown in Figure 16. Time constants to achieve 63.2% of the total temperature change of the liner are given in Figure 17 plotted against brake power as an indication of cylinder heat fluxes. Response times are a function of engine speed because the coolant pump is driven via the crankshaft through the FEAD.

The intake and exhaust valves are modelled as comprised of three elements: an upper stem, a lower stem and a valve head.

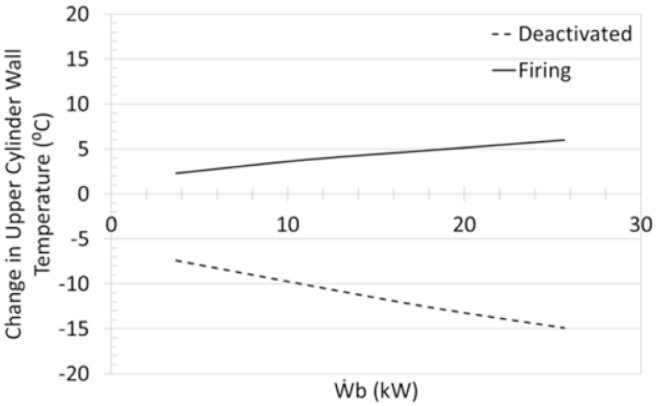

Figure 15. Modelled Cylinder #1 and #2 wall temperature (°C) changes for varying brake loads at an engine speed of 3500rpm.

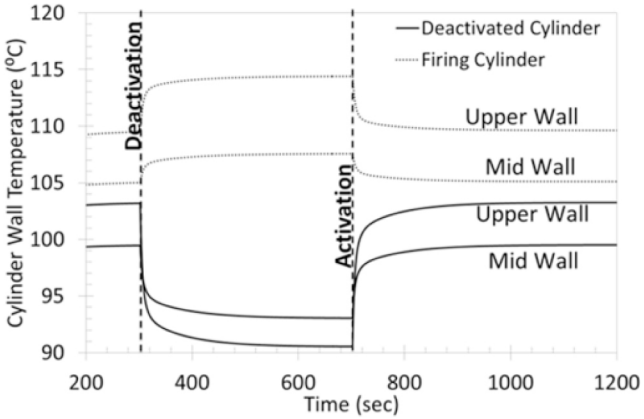

Figure 16. Example of modeled cylinder wall temperature change and response time; Tb = 50Nm, N = 3500rpm.

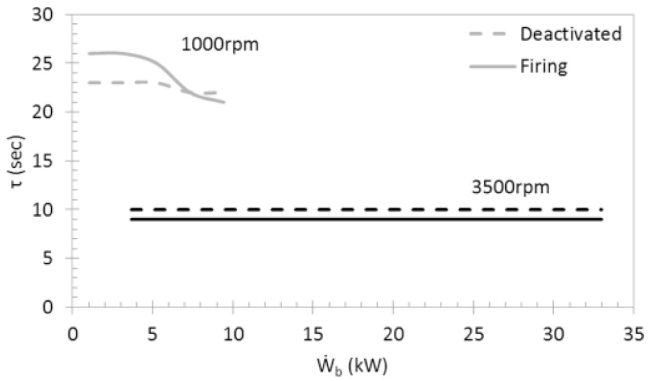

Figure 17. Modelled cylinder wall response time for two engine speeds N = 1000rpm and 3500rpm.

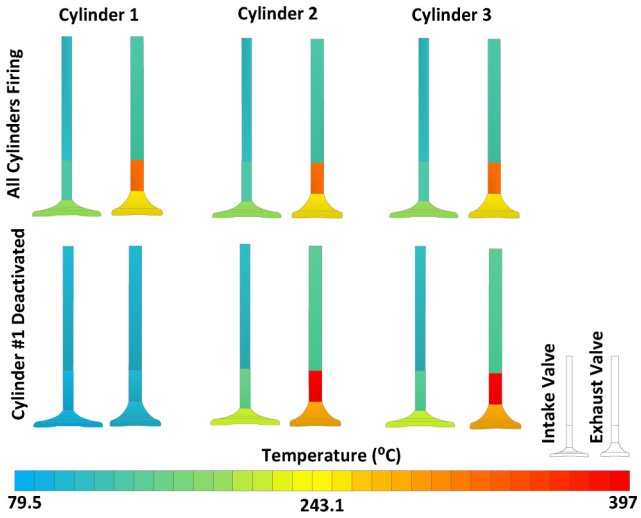

Figure 18. Modelled stabilised valve metal temperatures before and after deactivation; N=2000rpm and Tb= 60Nm.

The exhaust valves undergo larger temperature changes than the intake valves, and the largest temperature changes occur in the lower stems of the exhaust valves. An illustration of the steady- state valve temperatures before and after the deactivation of one cylinder is given in Figure 18. The changes in temperature of the exhaust valve lower stems are shown in Figure 19 as a function of engine brake power. The time constants for the changes are similar or shorter than those for the cylinder liner elements.

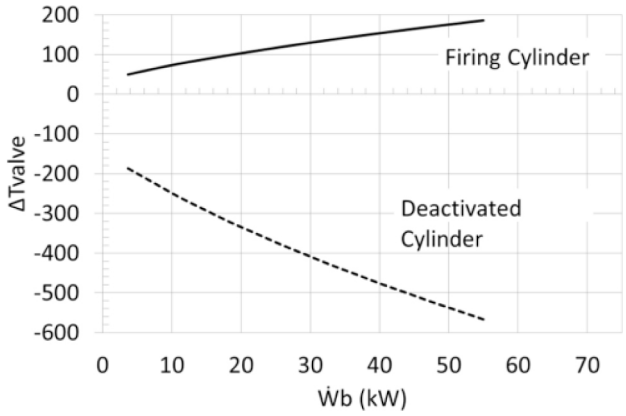

Figure 19. Modelled change in temperature for the exhaust valve lower stem component for the deactivated and firing cylinders at an engine speed of 3500rpm.

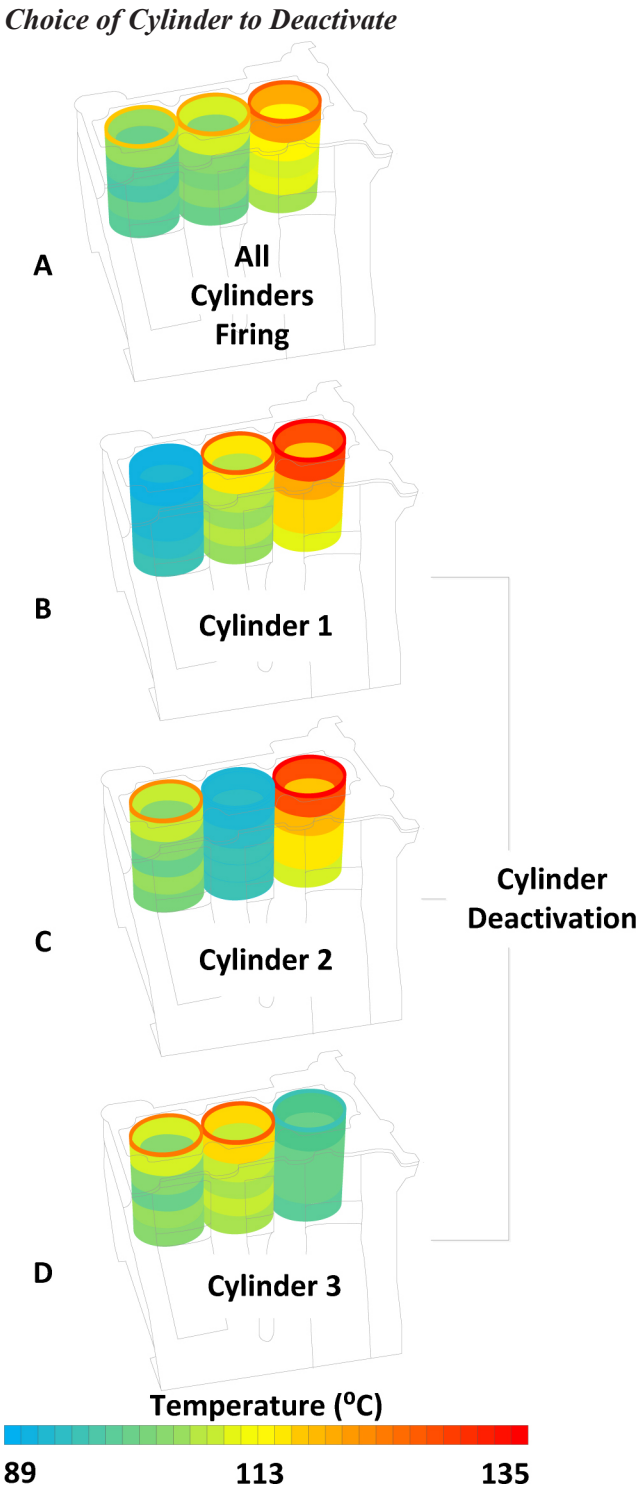

Figure 20. Modelled change in cylinder wall temperatures for VDE ON cases after deactivating [B] cylinder 1, [C] cylinder 2 and [D] cylinder 3 contrasted with [A] VDE OFF scenario (Tb = 60Nm, N = 2000rpm).

The choice of which cylinder to deactivate depends on range of thermal, dynamic and packaging considerations. The main thermal consideration is to minimise temperature differences between the deactivated and firing cylinders. For the coolant circuit illustrated in Figure 1, under fully warm operating conditions when firing on all cylinders, liner temperature increases in the direction of coolant flow as shown in Figure 20. When the coolest cylinder, Cylinder 1, is

deactivated the temperature differences between cylinders are maximised. These are similar when the centre cylinder is deactivated, and minimised when Cylinder 3 is deactivated. This last case takes advantage of the warmer coolant to minimise the temperature fall after deactivation, and the cooler coolant moderates the temperature rise in the firing cylinders. In principle applying deactivation to the hottest running cylinder, Cylinder 3 in this example, would be the preferred choice although dynamic and packaging considerations might dictate a compromise.

FUEL ECONOMY BENEFIT OF DEACTIVATION

The fuel economy benefit of cylinder deactivation over a cold-started drive cycle is derived from the reduction in pumping work and any improvement in cylinder indicated gross thermal efficiency. These are offset by the disadvantages of slower warm up and higher rubbing friction, and the penalty of motoring the deactivated cylinder. The largest reduction in fuel used over the drive cycle is achieved by allowing deactivation to occur from key-on, although this may not be practicable or desirable for other reasons: it slows engine warm-up, reduces the available heat input to the passenger compartment and slows the fall in rubbing friction with increasing oil temperature. If deactivation is permitted only when coolant temperature exceeds a minimum value, the fall in fuel saving with increasing threshold temperature is shown in Table 2 for the NEDC.

Table 2. Modelled delays in coolant and oil warm-up times over the NEDC and associated fuel consumption deterioration with the delays.

Coolant Temperature at which deactivation enabled (°C)	20	30	40	50	60	70	90 (fully warm)
Time for coolant to reach 90°C	1130	1116	989	971	944	900	882
Oil temperature when coolant reaches 90°C	87	89	84	84	82	81	79
Fuel consumption reduction over NEDC (%)	3.6	3.44	3.18	2.94	2.55	2.15	0.66

The predictions assume that once the threshold temperature is exceeded, deactivation is applied at engine loads up to 90Nm and all engine speeds and that gross indicated thermal efficiency is constant. Deactivation and reactivation events are assumed to take place instantaneously. The maximum fuel savings achieved by allowing deactivation from key-on are similar for the NEDC and FTP-75 cycle, at 3.6% and 3.5%. For ARTMIS and WLTC cycles, which are more dynamic and cover a wider range of engine loads, the predicted savings are smaller, at around 1% or less.

The predictions of fuel savings are robust to the upper limit on torque at which cylinder deactivation can be applied. In principle, the upper limit is set by the maximum work output provided by the two cylinders which continue to fire after the third has been deactivated, as this dictates the maximum engine torque that can be maintained. In practice, as engine torque increases the saving in pumping work diminishes and for the engine considered, above 90Nm it is small. Deactivation was allowed at all engine speeds. The speed boundaries set for the 1.4 litre TSI engine described in [2] are reported to be 1250 rpm to 4000rpm. The lower speed is the more restrictive limit, because it is close to the engine speeds associated with urban driving conditions. This can reduce the time spent operating with a cylinder or cylinders deactivated under conditions when deactivation would yield a significant fuel economy benefit [22].

CONCLUSIONS

A lumped thermal capacity model of a 1litre, 3 cylinder spark ignition engine has been developed and used to investigate thermal responses to deactivating one of the cylinders. On deactivation, the trapped cylinder charge reduces by typically 70% over 30 cycles; for the final conditions, the difference between gas compression and expansion work of the deactivated cylinder is typically 2-3J/rev and equivalent to ~0.02 bar net IMEP. The major loss of motoring the deactivated cylinder is the retained rubbing friction contribution.

On deactivating a cylinder, temperature differences between this and the adjacent cylinders increase. The largest differences are between elements at the top of the deactivated and firing cylinder liners and between the exhaust ports; the temperature differences are limited by the thermal coupling to coolant to a maximum of ~60 deg C. The largest temperature change is of the order of 350 deg C, in the exhaust vale lower stem of the deactivated cylinder. The time constants for temperature fields to adjust to new equilibrium temperatures are in the range of 10-30 seconds.

Simulated applications of cylinder deactivation over the NEDC and FTP-75 indicate fuel economy benefits of 3½% can be gained from reductions in pumping work if deactivation occurs on start up at 20°C. The benefit is lower for the more dynamic drive cycles such as ATEMIS and WLTC. The benefit is also reduced if deactivation is delayed until the coolant is fully warm; for the NEDC the fuel economy benefit is reduced to 2%.

REFERENCES

1. Ilhlemann A., Nitz N., *Cylinder Deactivation - A technology with a future or a niche application?*, 11th Schaeffler Symposium, 2014.
2. Middendorf H., Theobald J., Lang L., Hartel K., *The 1.4-L TSI Gasoline Engine with Cylinder Deactivation*, MTZ 03/2012, pp.186-193.
3. Friedfeldt R., Zenner T., Ernst R. and Fraser A.. *Three-Cylinder Gasoline: Engine with Direct Injection*. ATZ 02/2012, Volume 12, 2012.
4. Leone, T. and Pozar, M., "Fuel Economy Benefit of Cylinder Deactivation - Sensitivity to Vehicle Application and Operating Constraints," SAE Technical Paper 2001-01-3591, 2001, doi:10.4271/2001-01-3591.
5. Senapati, U., McDevitt, I., and Hankinson, A., "Vehicle Refinement Challenges for a Large Displacement Engine with Cylinder Deactivation Capability," SAE Technical Paper 2011-01-1678, 2011, doi:10.4271/2011-01-1678.

6. Fujiwara, M., Kumagai, K., Segawa, M., Sato, R. et al., "Development of a 6-Cylinder Gasoline Engine with New Variable Cylinder Management Technology," SAE Technical Paper 2008-01-0610, 2008, doi:10.4271/2008-01-0610.
7. Jost, Kevin, *Mercedes-Benz Launches Cylinder Cut-Out*, Automotive Engineering International Magazine, Jan. 1999.
8. Gush, B., Fleiss, M., Baron-Oxberry, S., Humpries, J., Seipel, T, Heritage, Technology, Torque: The All-New 6 3/4-V8 Turbo Engine For The Bentley Mulsanne. MTZ Worldwide, 2009. Volume 70, Issue 11, pp. 4-13.
9. Green Car Congress, "Ford Assessment of Two Cylinder Deactivation Strategies for Award-Winning 3-cyl. EcoBoost," http://www.greencarcongress.com/2015/06/20150623-schamel.html, accessed 12.03.2016.
10. Doller, S. Franke, S. Sengpiehl, Semper T., Activable Displacement SI Engine from IAV for CO2 Reduction, MTZ 12/2013, Volume 74.
11. Muhamad Said, M., Abdul Aziz, A., Abdul Latiff, Z., Mahmoudzadeh Andwari, A. et al., "Investigation of Cylinder Deactivation (CDA) Strategies on Part Load Conditions," SAE Technical Paper 2014-01-2549, 2014, doi:10.4271/2014-01-2549.
12. Watanabe, E. and Fukutani, I., "Cylinder Cutoff of 4-Stroke Cycle Engines at Part-Load and Idle," SAE Technical Paper 820156, 1982, doi:10.4271/820156.
13. Flierl R., Hannibal W., Schurr A., Neugartner J., Turbocharged Three-Cylinder Engine with Activation of A Cylinder, MTZ 06/2014.
14. Shayler, P., Christian, S., and Ma, T., "A Model for the Investigation of Temperature, Heat Flow and Friction Characteristics During Engine Warm-Up," SAE Technical Paper 931153, 1993, doi:10.4271/931153.
15. Shayler, P., Leong, D., and Murphy, M., "Contributions to Engine Friction During Cold, Low Speed Running and the Dependence on Oil Viscosity," SAE Technical Paper 2005-01-1654, 2005, doi:10.4271/2005-01-1654.
16. Shayler, P., Chick, J., and Ma, T., "Correlation of Engine Heat Transfer for Heat Rejection and Warm-Up Modelling," SAE Technical Paper 971851, 1997, doi:10.4271/971851.
17. Shayler, P., Chick, J., and Ma, T., "Effect of Coolant Mixture Composition on Engine Heat Rejection Rate," SAE Technical Paper 960275, 1996, doi:10.4271/960275.
18. Taylor, C.F. and Toong, T.Y. *Heat Transfer in Internal-Combustion Engines*. ASME Paper 57-HT-17, 1957.
19. Alkidas, A., "Effects of Operational Parameters on Structural Temperatures and Coolant Heat Rejection of a S. I. Engine," SAE Technical Paper 931124, 1993, doi:10.4271/931124.
20. Kuruppu, C., Pesiridis, A., and Rajoo, S., "Investigation of Cylinder Deactivation and Variable Valve Actuation on Gasoline Engine Performance," SAE Technical Paper 2014-01-1170, 2014, doi:10.4271/2014-01-1170.
21. Flierl, R., Lauer, F., Breuer, M., and Hannibal, W., "Cylinder Deactivation with Mechanically Fully Variable Valve Train," *SAE Int. J. Engines* 5(2):207-215, 2012, doi:10.4271/2012-01-0160.
22. McGhee, M., Bech, A., Shayler P.J. *Operation of cylinder deactivation of a 1.4l SI engine under real world driving conditions* Paper F2016-ESYA-012, FISITA 2016 World Automotive Congress, 26-30 September 2016, Busan, S. Korea

ACKNOWLEDGEMENTS

The authors thank the Advanced Propulsion Centre (APC) UK for funding this research as part of the ACTIVE project.

DEFINITIONS/ABBREVIATIONS

T_1 - Bottom Dead Centre Gas Temperature (Kelvin)

T_2 - Top Dead Centre Gas Temperature (K)

p_1 - Bottom Dead Centre Pressure (Pa)

p_2 - Top Dead Centre Pressure (Pa)

v_1 - Bottom Dead Centre Volume **(m^3)**

v_2 - Top Dead Centre Pressure **(m^3)**

ARTEMIS - Assessment and Reliability of Transport Emission Models and Inventory Systems

BDC - Bottom Dead Centre

BMEP - Brake Mean Effective Pressure (bar)

CAD - Computer Aided Design

CO2 - Carbon Dioxide

FEAD - Frontend Ancillary Drive

FTP-75 - Federal Test Procedure 75

GM - General Motors

IMAP - Intake Manifold Air Pressure

IMEP - Gross Indicated Mean Effective Pressure (bar)

m - Trapped charge mass (kg)

n - polytropic index

NEDC - New European Drive Cycle

PMEP - Pumping Mean Effective Pressure (bar)

PROMETS - Program for Modelling of Engine Thermodynamic Systems

Q - Heat Energy (Joules)

TSI - Turbocharged Stratified Ignition

V6 - Two three cylinder banks separated at an angle of 60°

VW - Volkswagen

W - Work Energy (Joules)

WLTC - World Harmonised Light Duty Vehicle Test Procedure

γ - adiabatic index

APPENDIX

APPENDIX 1

WORK DONE ON THE GAS IN THE DEACTIVATED CYLINDER

Work done *on* the gas during the compression process:

$$\boldsymbol{W = -m\int_1^2 pdv = -m(p_2v_2 - p_1v_1)/(1-n)}$$

First Law for a closed system applied to the cylinder, with heat transfer *from* the gas taken to be positive

$$W = Q + \Delta U$$

and

$$Q = -\frac{m(p_2v_2 - p_1v_1)}{1-n} - mc_v(T_2 - T_1)$$

$$Q = mR(T_2 - T_1)\left(\frac{\gamma - n}{(n-1)(\gamma-1)}\right)$$

If the temperature change over the expansion is the same as during the compression, then over the compression and expansion strokes of one engine revolution:

$$\oint W = -\oint Q_{rev,n} = -2mR\Delta T\left(\frac{\gamma-n}{(\gamma-1)(n-1)}\right)$$